Ab Initio Study of Water Adsorption on α-Al_2O_3 (0001) Crystal Surface

Vladimir Shapovalov and Thanh N. Truong*

Henry Eyring Center for Theoretical Chemistry, Department of Chemistry, University of Utah, 315 South 1400 East, Rm 2020, Salt Lake City, Utah 84112

Received: April 13, 2000; In Final Form: July 25, 2000

Ab Initio embedded cluster calculations were performed to study water adsorption on Al-terminated (0001) α-Al_2O_3 surface. We used the surface charge representation of the embedding electrostatic potential (SCREEP) model to give an accurate representation of the Madelung potential at the adsorption site. The geometry of the cluster was optimized to take into account the surface relaxation. Adsorption energies were obtained using the *N*-layer integrated molecular orbital model (ONIOM). In the case of water adsorption it was found that both dissociative and molecular adsorption minima exist, with adsorption energies of −31.57 and −23.40 kcal/mol, respectively, in agreement with experiment. Bond orders, covalences and full atomic valences were analyzed to investigate the changes in the chemical bonding during adsorption. Our results provide some insight into the scrambling of water and crystal oxygen atoms during water desorption in isotopic exchange experiments.

1. Introduction

Research related to aluminum oxide is motivated by extensive use of this material and by its role in environmental chemistry. One of the major industrial applications of aluminum oxide is its use as a catalyst and a catalyst support.[1] It is also employed to grow insulator and semiconductor films for microelectronics.[2] An aluminum oxide coat is commonly formed on the surface of Al-based lightweight construction materials.[3] In nature this compound can be found as a component of soil.[4] Another source of aluminum oxide in the environment is the Al(III) salts used for treatment of industrial wastewater and municipal sewage.[5] In the atmosphere concentration of dispersed alumina has increased by a factor of 20 during the period from 1976 to 1984.[6] Most of this increase was attributed to the use of metallic aluminum in solid rocket motors. Thus, hundreds of tons of dispersed alumina are discharged into the atmosphere during each space shuttle launch.[7] Interaction of the alumina surface with water and its hydroxylation is of primary importance in all these fields.

The majority of experiments was performed on powders (e.g., Rossi et al.,[8] Bagane et al.,[9] McHale et al.[10]). These results have very little use in microscopic interpretations, since the adsorption sites are not well defined. Water adsorption energies in these experiments were found in the broad range from 8 to 64 kcal/mol. Recently, a study on the α-Al_2O_3 (0001) single-crystal surface was conducted by Nelson et al.[11] Dissociative adsorption of water was clearly observed and the binding energy was found to be 25−40 kcal/mol. In addition, a complete scrambling of the crystal and water oxygen atoms was observed in isotopic exchange experiments performed by the same group.[12]

Previous theoretical studies of the surface reactivity toward water and of the surface hydroxyls properties employed both empirical and quantum-mechanical methods.[13−17] Bargar et al.[13] employed an empirical model based on the band valence concept to predict the relative stability of different kinds of adsorbed species on the alumina surface in an aqueous solution. Unfortunately, their predictions were only qualitative. In a paper by Nygren et al.[15] water desorption energy was evaluated by an ab initio embedded cluster method. A rather small cluster $Al(OH)_3$ embedded in the field of point charges was used in such a study. The desorption energy was found in the range from 120 to 254 kcal/mol, depending on the values of the embedding charges. A more accurate ab initio calculation was performed by Wittbrodt et al.[16] They also used an embedded cluster approach. A larger cluster was used to allow different configurations of adsorbed species. However, in calculations of surface relaxation as well as adsorption, the positions of the pure ion point charges representing the Madelung potential were fixed at positions corresponding to the unrelaxed surface, and cutoff functions had to be employed to approximate the Madelung potential. The reported binding energies vary with the methods and basis sets used but are mostly within the experimental range (23−41 kcal/mol). A periodic ab initio MD simulation based on the Car-Parrinello methodology was performed by Hass et al.[17] They studied a periodic slab at different water coverage. Both molecular and dissociative adsorption was considered. In the case of dissociative adsorption two pathways for the proton transfer were investigated: 1−2 dissociation (proton transfer to the nearest crystal oxygen) and 1−4 dissociation (proton transfer to the second nearest oxygen). In agreement with the previous embedded cluster study by Wittbrodt et al.[16] 1−4 dissociation was predicted to have a lower barrier, and thus to be more kinetically favorable. The binding energy for 1−4 adsorption of 32.5 kcal/mol is slightly smaller than 33.2 kcal/mol for the 1−2 dissociative adsorption. The binding energy for molecular adsorption was predicted to be 23.3 kcal/mol in that study.

Despite rapidly increasing computer speeds, the modern level of computational resources still restricts one to considering systems of a very limited size for practical applications. In this respect the development of cost-effective models for studying surfaces and interfaces is essential. The ONIOM[18] model was shown to achieve this goal by treating a small region that is critical to the chemistry at a high level of theory, while treating the remaining region at a less accurate level. This model so far has been applied to isolated systems. In this paper we illustrate

10.1021/jp001399g CCC: $19.00
Published on Web 09/27/2000

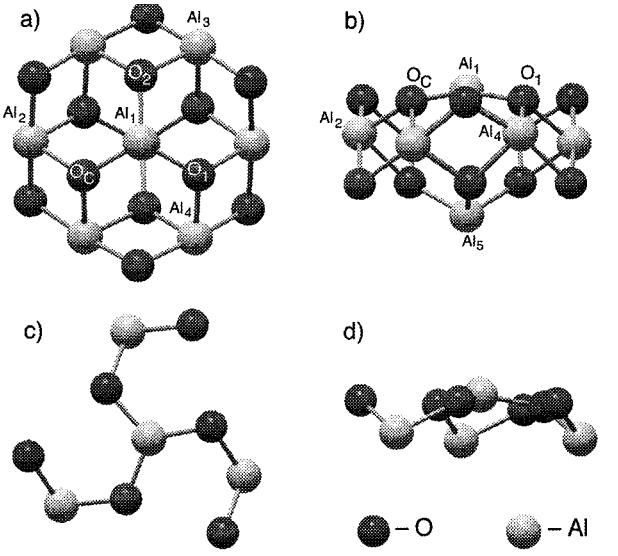

Figure 1. Top (a) and side (b) views of the real system and top (c) and side (d) views of the model system.

how the ONIOM model can be employed to study water adsorption on an aluminum oxide surface.

In the present study we have two objectives: (1) to investigate the applicability of the ONIOM model in studies of the adsorption processes on a crystal surface and (2) to investigate the chemistry of water adsorption on the Al_2O_3 (0001) surface.

2. Computational Details

To achieve the optimal level of computational accuracy for a given amount of computational resources we employ an embedded cluster model within the ONIOM methodology. In particular, we used a two-layer model where both layers are treated at different molecular orbital levels of theory (IMOMO).[19,20] In this approach two systems are considered: the larger real system treated at a lower and less computationally expensive level of theory, and a smaller model system treated at the same level as the real system, and also a higher level of theory. Then, an estimate of the total energy of the real system at the higher level of theory can be expressed as

$$E_{\text{real,high}} \cong E_{\text{real,low}} - E_{\text{model,low}} + E_{\text{model,high}} \qquad (1)$$

In this case, to calculate $E_{\text{real,low}}$ the real system is divided into three regions: the inner, the intermediate, and the outer ones. The inner region consists of the adsorbate and of a cluster representing the adsorption site. Interaction in this region is modeled quantum mechanically. In principle, one should use a large cluster to minimize the boundary effects at the adsorption site. However, selecting the size of the quantum (QM) cluster is dictated by the balance between accuracy and computational demand. To optimize this cost/performance ratio, we select the quantum cluster to be Al_8O_{12} (see Figure 1a,b) plus the adsorbate (a water molecule). This QM cluster is treated at the MP2 level of theory. LANLDZ[21] basis functions with pseudopotentials were used for Al atoms, with a set of d functions added on the adsorption site Al atom, and all-electron 6-31G(d,p) basis was used for O atoms and for the adsorbate. The intermediate region of the real system is designed to prevent leakage of the electronic density of the QM cluster to the outer region. This is done by treating all Al atoms closest to the QM cluster as whole ion LANL[21] pseudopotentials. Finally, the outermost region is treated classically and is designed to accurately describe the Madelung potential of the crystal surrounding the QM cluster. This is done by representing a small number of lattice atoms near the QM cluster as point charges. The Madelung potential due to the remaining crystal is described by the surface charge representation of external embedding potential (SCREEP) method.[22] This embedding provides highly accurate representation of the Madelung potential of the infinite crystal using a relatively small number of point charges. The values of the atomic charges used to evaluate the Madelung field of the ideal crystal were taken from a periodic calculation by Puchin et al.[23]

The model system for calculating $E_{\text{model,high}}$ and $E_{\text{model,low}}$ is represented by a smaller cluster Al_4O_6 (see Figure 1c,d) with the adsorbed water with no embedding pseudopotentials or point charges. The CCSD level of theory was selected as the high level treatment with the same basis set as described above for the low level.

The position of the adsorption site Al atom and the geometry of chemisorbed and physisorbed water molecule were optimized at the MP2 level of theory. In the case of dissociative adsorption only 1−2 process (proton transfer to the nearest oxygen atom) was considered. Single point energy calculations using the IMOMO methodology were carried out to improve the energetic information. Population analysis was performed on the symmetrically orthogonalized MP2 wave function[24] for the real system. During the population analysis the polarization functions on the adsorption site Al were excluded so that balanced electron density distribution could be obtained. We used the population analysis introduced by Evarestov and Veryazov[25] to calculate total valence, covalence, bond order, and atomic charge of the QM cluster. This analysis was shown to discriminate extremely well the total valence of atoms in different valent states, such as Pb(II) and Pb(IV); Cu(I), Cu(II), and Cu(III); Ti(II) and Ti(IV).[25−27] The density of states (DOS) graphs were obtained by broadening the orbital energy levels with Gaussian functions with width of 1 eV at half-maximum. The changes in the DOS spectrum as a water molecule is absorbed provide useful qualitative information that can be compared with UPS and MIES experiments.

All calculations were done using our locally modified GAUSSIAN98/DFT computer code.[28]

3. Results and Discussion

We first discuss the structure of the Al-terminated (0001) surface of α-Al_2O_3. This surface is well characterized and has been extensively studied by both experimental and theoretical methods. Although there are three possible terminations of the (0001) surface (Figure 2), we used the Al-terminated surface (termination 3 in Figure 2) for the following reasons: (1) this termination was predicted to be the most stable in a vacuum in several previous theoretical studies;[29,30] (2) it is also consistent with experimental findings that the stoichiometric composition of the three topmost layers is Al_4O_3,[31] and that Al atoms are located above the oxygen plane.[32] Previous theoretical calculations[16,23,33] yielded large, though quite different, relaxation values, ranging from 68 to 86%. This finding was confirmed experimentally by Ahn and Rabalais.[32] In this study we illustrated that such a large surface relaxation can be modeled by the embedded cluster methodology in a self-consistent manner. Since the changes in the oxygen layer during relaxation previously were found to be much smaller than those of the surface aluminum layer,[16] only the positions of the surface aluminum atoms were optimized here. The embedding environment was adjusted to preserve the periodic structure consistent with the optimized structure of the cluster. The height of Al above the oxygen plane was found to be 0.246 Å (70.4%

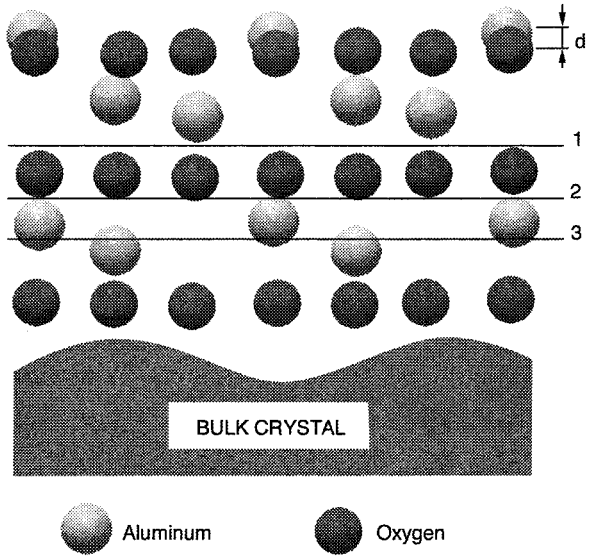

Figure 2. Various terminations of (0001) surface of α-Al_2O_3: (1) oxygen termination, negatively charged surface; (2) aluminum termination, positively charged surface; (3) aluminum termination, neutral surface. Surface relaxation is measured as percent decrease of the *d* value, the distance between the Al and O planes.

TABLE 1: Charges (*Q*), Covalences (*C*), and Valences (*V*) of the Cluster Atoms

		Q	*C*	*V*
bare surface	Al_1	1.29	2.74	3.26
	$Al_{2,3,4}$	1.57	2.33	3.12
	Al_5	1.77	2.03	3.05
	O	−0.84	1.94	2.25
molecular adsorption	Al_1	1.20	2.88	3.32
	O_C	−0.87	1.90	2.24
	O_W	−0.52	2.11	2.23
dissociative adsorption	Al_1	1.32	2.80	3.33
	$O_{1,2}$	−0.92	1.88	2.26
	O_C	−0.71	2.13	2.34
	O_W	−0.80	1.81	2.11

TABLE 2: Bond Lengths (Å) and Bond Orders

	bond	bond length	bond order
bare surface	Al_1-O	1.68	0.73
molecular adsorption	$Al_1-O_{1,2}$	1.72	0.63
	Al_1-O_C	1.70	0.70
	Al_1-O_W	1.99	0.40
	O_W-H_1	0.99	0.79
	O_W-H_2	0.98	0.81
dissociative adsorption	$Al_1-O_{1,2}$	1.72	0.65
	Al_1-O_C	2.00	0.29
	Al_1-O_W	1.75	0.78
	O_W-H_W	0.97	0.88
	O_C-H_C	0.99	0.77

relaxation), which compares favorably with the experimental estimate of 0.3 ± 0.1 Å,[32] and 0.25 Å as obtained in a similar calculation of Wittbrodt et al.[16] Periodic Car-Parrinello calculation by Hass et al.[17] predicted a larger relaxation of 82%, which results in the distance between the Al and O layers of about 0.15 Å.

We further analyzed the electronic structure of the surface in order to investigate the effect of surface relaxation. The local electronic characteristics of the cluster atoms are given in Table 1 and Table 2. The Al charge is 1.29 au for the exposed atom (Al_1 in Figure 1a,b), and 1.57 au for the inner atoms (Al_2-Al_4) while the covalence is 2.74 and 2.33, respectively. The increase in the covalence of the surface atoms and their abnormally high valence indicate an excess of electronic density available for

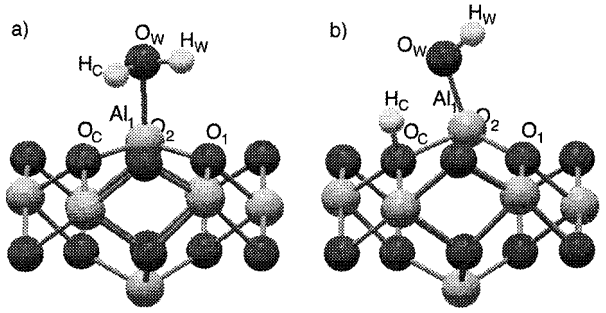

Figure 3. Optimized geometry of water adsorbed on the real model in molecular (a) and dissociative (b) configurations.

binding of the adsorbed species. This is undoubtedly a surface phenomenon and is not an artifact of the cluster model. One can confirm this by noting the valence of the Al_5 atom, which is also located on the edge of the cluster but in the bulk and has different surrounding, to have a typical value of 3.05.

Adsorption of water was found to have noticeable effects on both geometry and electronic structure of the underlying crystal (Figure 3) even though the charge and total valence of the Al adsorption site do not change much during either molecular or dissociative adsorption (see Table 1). During adsorption the distance between the oxygen plane and the aluminum atom increases, which was also observed in the study by J. M.Wittbrodt et al.[16] In our calculations the surface relaxation decreased by 22.3% during molecular adsorption and by 56.9% during dissociative adsorption. We found that Al_1 atom during the adsorption process shifts not only perpendicularly to the surface, but also sideways; consequently the three formerly identical Al_1-O_C, Al_1-O_1, and Al_1-O_2 bonds become different (Table 2). Here Al_1 and O_C are the adsorption sites. The differences are about 0.02 Å for molecular adsorption. However, for the dissociative adsorption the Al_1-O_C bond distance is significantly elongated to 2.00 Å as compared to 1.72 Å for the other two Al_1-O bonds. The large differences in the Al_1-O bonds up on dissociative adsorption can also be seen in the bond order analysis. Their bond orders differ by more than a factor of 2, namely, 0.65 au for the shorter Al_1-O_1 and Al_1-O_2 bond, and 0.29 au for the longer Al_1-O_C bond. Compared with the initial (prior to adsorption) value of 0.73 au, the Al_1-O_C bond is 2.5 times weaker.

A closer look at the population analysis for the dissociative adsorption case yields an interesting observation. The charge of the O_C atom decreases to −0.71 from −0.84. It is significantly lower than charges of other surface oxygen atoms O_1 and O_2 (−0.92), and is closer to the charge on O_W (−0.80). Note that the O_c atom was not relaxed in this case. However, as mentioned earlier that the oxygen sublayer was previously found to have very small relaxation,[16] thus we do not expect relaxing the O_c would change the general observation here. The orders of OH bonds are also close for the two hydroxyls: 0.88 for O_WH_W and 0.77 for O_CH_C. These results indicate that the local electronic structure and chemical bonding of the surface oxygen O_C and the adsorbed oxygen O_W are very similar. This similarity provides some initial insight for the observation of nearly 50/50 scrambling of oxygen atoms originating from water and crystal in Elam et al.'s isotopic exchange experiments.[12] However, to fully understand such an experimental observation, more detailed analysis on the mechanism of the water desorption process is required.

Calculated adsorption energies are listed in Table 3 along with experimental and previous theoretical results. We found the adsorption energy to be −28.32 kcal/mol for molecular

TABLE 3: Adsorption Energies (kcal/mol)

model	method	molecular adsorption	dissociative adsorption
experiment		not observed	-(23−41)
theory			
$Al(OH)_3$ embedded cluster[a]	HF	n/a	-(120−254)
Al_8O_{12} embedded cluster[b]	HF	−35.7	−59.4
Al_8O_{12} cluster[c]	B3LYP	−31.62	−32.14
periodic Al_2O_3[d]	Periodic BLYP	−23.3	−33.2
Al_4O_6 cluster	MP2	−40.32	−37.01
Al_4O_6 cluster	CCSD	−33.20	−34.97
Al_8O_{12} embedded cluster	MP2	−35.43	−37.82
Al_8O_{12} cluster[e]	MP2	−40.18	−33.18
(Al_4O_6: $Al_{l8}O_{12}$ emb cluster)[f]	(CCSD:MP2)	−28.32	−35.78
(Al_4O_6: $Al_{l8}O_{12}$ emb cluster)[f]	(CCSD:MP2) + BSSE	−23.40	−31.57

[a] From ref 15 SCF level of theory with modified coupled pair potential. [b] From ref 16 6-31+G* basis set was used on the central atoms of the cluster, 3-21G on the rest of atoms. Cluster was embedded in the field of point charges. [c] From ref 16 Same basis set as in b) but without embedding. [d] From ref 17 Periodic slab BLYP Car-Parrinello simulation. [e] Cluster calculations at the MP2 embedded cluster geometries. [f] IMOMO calculations. CCSD calculations for the model system (Al_4O_6 cluster) and MP2 calculations for the real system (Al_8O_{12} embedded cluster).

adsorption, and −35.78 kcal/mol for dissociative adsorption. Including basis set superposition errors estimated by the counterpoise method raises the molecular adsorption energy to −23.40 kcal/mol, and dissociative adsorption energy to −31.57 kcal/mol. Our prediction agrees well with the experimental estimate[11] between −23 and −41 kcal/mol. The fact that dissociative adsorption is more stable correlates well with the results of isotopic exchange experiments (ref 11). The calculated adsorption energies are significantly less negative than those of Nygren et al.[15] In the latter work it was assumed the alumina surface is completely hydroxylated, whereas our calculations correspond to the low coverage condition. Our adsorption energies are much closer to the upper limit of those obtained by Wittbrodt et al.,[16] where the same quantum cluster was used but at different levels of theory. It is interesting to note that our results are within less than 1.7 kcal/mol from those of the periodic slab Car-Parrinello study.[17]

Analysis of the contributions of different component of the IMOMO scheme is also listed in Table 3. This provides an interesting insight into the physical system and theoretical method used. The result that attracts the most attention is that the model system treated as a bare cluster at the MP2 level gives qualitatively wrong relative adsorption energies (molecular lower than dissociative). The same system treated at the CCSD level gives quantitatively acceptable results. One may suggest that the MP2 method with relatively small basis does not accurately estimate correlation effect in this system. However, the real system treated at the MP2 level gives correct relative positions of the molecular and dissociative minima, though their numeric values are underestimated. Note that there are two differences in the MP2 calculations for the model and the real systems, namely the larger quantum cluster size and inclusion of the Madelung field in the real system. To understand the effects of the Madelung field on the adsorption energies, we have also calculated single-point MP2 calculations for the real system but without the Madelung field using the MP2 embedded-cluster optimized structures. The Madelung field was found to raise the adsorption energies by 4.75 kcal/mol for the molecular adsorption while lower it by 4.64 kcal/mol for the dissociative adsorption. These results are consistent with those from Wittbrodt et al.[16] Thus, our results suggest that the correlation effects and electrostatic effects are important for the correct order of the relative adsorption energies. It is interesting to note that a similar behavior, when the model system gave a qualitatively wrong result at the lower level of treatment, was previously observed in a calculation of the transition state for an S_N2 reaction,[19] and was also attributed to the underestimated electronic correlation effects.

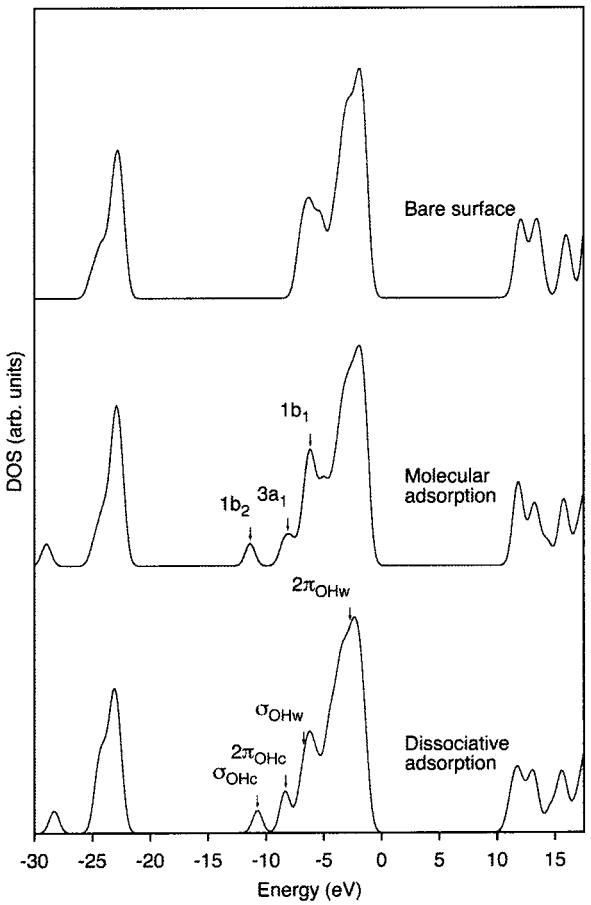

Figure 4. Calculated MP2 DOS for the bare cluster and clusters with molecularly and dissociatively adsorbed water. Cluster states originating from molecular orbitals of water and hydroxyl are labeled. OH_C refers to the hydroxyl formed with the oxygen of the alumina surface, and OH_W to the hydroxyl with the oxygen of the water molecule.

Since electronic spectra may provide assistance in determining the nature of the surface species, we also performed analysis of the DOS. The calculated DOS is shown in Figure 4, and the positions of the states due to the adsorbed water are given in Table 4. The zero of energy corresponds to the top of the valence band. The O(2s) states are found in the region from −21 to −30 eV. The valence band of the bare cluster shows two peaks with shoulders. The lower peak and its shoulder are the bonding

TABLE 4: Positions of the DOS Bands Relative to the Valence Band Maximum (eV)

	H_2O		O_WH_W	O_CH_C
$1b_2$	−11.35	σ	−6.76	−10.75
$3a_1$	−8.10	π_1	−2.73	−8.50
$1b_1$	−6.17	π_2	−2.43	−8.18

orbitals formed by O(2p) and Al(3s) atomic orbitals, and the upper peak and its shoulder are the nonbonding O(2p) orbitals.

The new feature resulting from water adsorption, common to both molecular and dissociative adsorptions are the two peaks between −13 and −7 eV. Although these spectra look very similar, the nature of these orbitals is quite different. Atomic orbitals of the adsorbed species are somewhat mixed with the cluster orbitals, but still can be traced back to the molecular orbitals from which they originate. In the spectrum of molecularly adsorbed water the orbitals are classified according to the irreducible representations of the water molecule point group. The states between −13 and −7 eV are formed mostly by O_W(2p) and H(1s) orbitals. On the basis of the analysis of the orbital coefficients we give the following assignments: the peak at −11.35 eV is almost entirely $1b_2$ orbital of water; the peak at −8.10 eV is mostly the $3a_1$ water molecule orbital, and the $1b_1$ water orbital is found within the peak with maximum at −6.17 eV. It is slightly hybridized with the aluminum oxide states and is responsible for the chemical bonding of water to the surface.

In the spectrum of dissociatively adsorbed water one would expect to find six subbands from the two OH_W, and OH_C hydroxyl groups. Each hydroxyl group would produce orbitals originating from the bonding σ orbital and two nonbonding π orbitals. The orbitals of the OH_C hydroxyl group will probably be shifted downward with respect to OH_W hydroxyl due to the positive crystal potential on O_C, thus resulting in total of six states. Instead, we find the picture very similar to that of the molecular adsorption. The analysis of the orbital coefficients shows that the singlet with the maximum at −10.75 eV is made up of almost exclusively O(2p) and H(1s) states, and thus can be assigned to the σ orbital of the hydroxyl formed by the surface oxygen and H_w. The peak at −8.50 eV with the area twice that of the σ orbital is the two nonbonding π orbitals of the same hydroxyl group. Its small width is also an indication that the hydroxyl's state is not very much perturbed by the surface. This observation also contributes to the explanation why this hydroxyl can desorb as easily as O_WH_W. The next two peaks at −6.76 eV (σ) and about −2.5 eV (π) are assigned to σ and π orbitals of the O_WH_W group. These orbitals are strongly hybridized with the aluminum oxide states.

4. Conclusions

Ab initio embedded cluster calculations within the ONIOM methodology were performed to study the adsorption of water on α-Al_2O_3 (0001) surface. Two energy minima corresponding to molecular (−23.4 kcal/mol) and dissociative (−31.57 kcal/mol) adsorption were found. Dissociative adsorption was found to be preferred in agreement with experiment observation. During dissociative adsorption extensive changes in the chemical bonding were found. Population analysis on the dissociative adsorption shows that charge and bonding characteristics of the adsorbed water and surface oxygen become very similar. This provides some insight into the 50/50 oxygen scrambling in isotopic exchange experiments. Further study on different water desorption pathways is needed to give full understanding of such scrambling process.

Acknowledgment. This work was supported in part by the National Science Foundation. Computer time was provided in part by Center for High Performance Computing (CHPC) at the University of Utah. CHPC's SGI Origin 2000 system is funded in part by the SGI Supercomputing Visualization Center Grant. We would like to thank Prof. S. M. George and Prof. H. B. Schlegel for useful discussions.

References and Notes

(1) Knozinger, H.; Ratnasamy, P. *Catal. Rev.—Sci. Eng.* **1978**, *17*, 31.
(2) Dorre, E. *Alumina: Processing Properties and Applications*; Springer-Verlag: New York, 1984.
(3) de SainteClaire, P.; Hass, K. C.; Schneider, W. F.; Hase, W. L. *J. Chem. Phys.* **1997**, *106*, 7331.
(4) Coston, J. A.; Fuller, C. C.; Davis, J. A. *Geochim. Cosmochim. Acta* **1995**, *59*, 3535.
(5) Hayden, P. L.; Rubin, A. J. *Aqueous-environmental chemistry of metals*; Ann Arbor Science: Ann Arbor, MI, 1974.
(6) Zolensky, M. E.; McKay, D. S.; Kaczor, L. A. *J. Geophys. Res.* **1989**, *94*, 1047.
(7) Cofer, III, W. R.; Lala, G. G.; Wightman, J. P. *Atmos. Environ.* **1987**, *21*, 1187.
(8) Rossi, P. F.; Oliveri, G.; M. Bassoli, M. *J. Chem. Soc., Faraday Trans.* **1994**, *90*, 363.
(9) Bagane, M.; Gannouni, A. *Ann. Chim.* **1995**, *20*, 72.
(10) McHale, J. M.; Auroux, A.; Perrotta, A. J.; Navrotsky, A. *Science* **1997**, *277*, 788.
(11) Nelson, C. E.; Elam, J. W.; Cameron, M. A.; Tolbert, M. A.; George, S. M. *Surf. Sci.* **1998**, *416*, 341.
(12) Elam, J. W.; Nelson, C. E.; Cameron, M. A.; Tolbert, M. A.; George, S. M. *J. Phys. Chem. B* **1998**, *102*, 7008.
(13) Bargar, J. R.; Brown, G. E.; Parks, G. A. *Geochim. Cosmochim. Acta* **1997**, *61*, 2617.
(14) Kawakami, H.; Yoshida, S. *J. Chem. Soc., Faraday Trans.* **1985**, *81*, 1117.
(15) Nygren, M. A.; Gay, D. A.; Catlow, C. R. A. *Surf. Sci.* **1997**, *380*, 113.
(16) Wittbrodt, J. M.; Hase, W. L.; Schlegel, H. B. *J. Phys. Chem. B* **1998**, *102*, 6539.
(17) Hass, K. C.; Schneider, W. F.; Curioni, A.; Andreoni, W. *Science* **1998**, *282*, 265.
(18) Svensson, M.; Humbel, S.; Froese, R. D. J.; Matsubara, T.; Sieber, S.; Morokuma, K. *J. Phys. Chem.* **1996**, *100*, 19357.
(19) Svensson, M.; Humbel, S.; Morokuma, K. *J. Chem. Phys.* **1996**, *105*, 3654.
(20) Humbel, S.; Sieber, S.; Morokuma, K. *J. Chem. Phys.* **1996**, *105*, 1959.
(21) Wadt, W. R.; Hay, P. J. *J. Chem. Phys.* **1985**, *82*, 1.
(22) Stefanovich, E. V.; Truong, T. N. *J. Phys. Chem. B* **1998**, *102*, 3018.
(23) Puchin, V. E.; Gale, J. D.; Shluger, A. L.; Kotomin, E. A.; Guenster, J.; Brause, M.; Kempter, V. *Surf. Sci.* **1997**, *370*, 190.
(24) Loewdin, P. *Adv. Quantum Chem* **1970**, *5*, 185.
(25) Evarestov, R. A.; Veryazov, V. A. *Theor. Chim. Acta* **1991**, *81*, 95.
(26) Evarestov, R. A.; Tupitsyn, I. I.; Veryazov, V. A. *Int. J. Quantum Chem* **1994**, *52*, 295.
(27) Evarestov, R. A.; Leko, A. V.; Veryazov, V. A. *Phys. Stat. Sol (b)* **1997**, *203*, R3.
(28) Frisch, M. J.; Trucks, G. W.; Schlegel, H. B.; Scuseria, G. E.; Robb, M. A.; Cheeseman, J. R.; Zakrzewski, V. G.; Montgomery, J. A., Jr.; Stratmann, R. E.; Burant, J. C.; Dapprich, S.; Millam, J. M.; Daniels, A. D.; Kudin, K. N.; Strain, M. C.; Farkas, O.; Tomasi, J.; Barone, V.; Cossi, M.; Cammi, R.; Menucci, B.; Pomelli, C.; Adamo, C.; Clifford, S.; Ochterski, J.; Petersson, G. A.; Ayala, P. Y.; Cui, Q.; Morokuma, K.; Malick, D. K.; Rabuck, A. D.; Raghavachari, K.; Foresman, J. B.; Cioslowski, J.; Ortiz, J. V.; Baboul, A. G.; Stefanov, B. B.; Liu, G.; Liashenko, A.; Piskorz, P.; Komaromi, I.; Gomperts, R.; Martin, R. L.; Fox, D. J.; Keith, T.; Al-Laham, M. A.; Peng, C. Y.; Nanayakkara, A.; Gonzalez, C.; Challacombe, M.; Gill, P. M. W.; Johnson, B.; Chen, W.; Wong, M. W.; Andres, J. L.; Gonzalez, C.; Head-Gordon, M.; Replogle, E. S.; Pople, J. A. *Gaussian 98*, Revision A.7; Gaussian, Inc.: Pittsburgh, PA, 1998.
(29) Ellis, D. E.; Guo, J.; Lam, D. J. *J. Am. Chem. Soc.* **1994**, *77*, 398.
(30) Blonski, S.; Garofalini, S. H. *Surf. Sci.* **1993**, *295*, 263.
(31) Gillet, E.; Ealet, B. B. *Surf. Sci.* **1992**, *273*, 427.
(32) Ahn, J.; Rabalais, J. W. *Surf. Sci.* **1997**, *388*, 121.
(33) Manassidis, I.; De Vita, A.; Gillan, M. J. *Surf. Sci. Lett.* **1993**, *285*, L517.